



HAL
open science

Characterising the behaviour of workpieces under the effect of tangential cutting force during NC turning

Stephane Segonds, Guillaume Cohen, Yann Landon, Frederic Monies, Pierre Lagarrigue

► **To cite this version:**

Stephane Segonds, Guillaume Cohen, Yann Landon, Frederic Monies, Pierre Lagarrigue. Characterising the behaviour of workpieces under the effect of tangential cutting force during NC turning: Application to machining of slender workpieces. *Journal of Materials Processing Technology*, 2006. hal-03832299

HAL Id: hal-03832299

<https://hal.science/hal-03832299>

Submitted on 27 Oct 2022

HAL is a multi-disciplinary open access archive for the deposit and dissemination of scientific research documents, whether they are published or not. The documents may come from teaching and research institutions in France or abroad, or from public or private research centers.

L'archive ouverte pluridisciplinaire **HAL**, est destinée au dépôt et à la diffusion de documents scientifiques de niveau recherche, publiés ou non, émanant des établissements d'enseignement et de recherche français ou étrangers, des laboratoires publics ou privés.

Characterising the behaviour of workpieces under the effect of tangential cutting force during NC turning

Application to machining of slender workpieces

Stephane Segonds*, Guillaume Cohen, Yann Landon, Frederic Monies, Pierre Lagarrigue

Laboratoire de Génie Mécanique de Toulouse, Bât.3R1, Université Paul Sabatier, 118 Rte de Narbonne, 31062 Toulouse Cedex 4, France

Received 3 March 2004; received in revised form 5 July 2005; accepted 23 August 2005

Abstract

Turning slender workpieces usually means a tailstock centre has to be used in order to achieve geometric tolerances for cylindricity. Indeed, tight tolerances mean the grinding phase can be performed quicker or even rendered superfluous. To limit use of the tailstock centre, that limits tool access when producing slender workpieces using turning, knowledge of the spindle–chuck–workpiece assembly's behaviour is essential. It is proposed to characterise this assembly's behaviour under the action of machining loads in order to introduce a method that in some cases will dispense with the need to use the tailstock centre while keeping the geometric quality of the machined workpiece.

Keywords: NC turning; Flexure; Slender workpieces; Compensation

1. Introduction

Turning slender workpieces generally means a tailstock centre has to be used to limit workpiece flexure during machining. Jig boring has to be implemented first at one end of the workpiece, possibly over a machining oversize that will have to be removed later. Using the tailstock centre thus leads firstly to additional operations to prepare workpieces with the increased production cost this entails. Secondly, its presence limits access to one end of the workpiece and can prevent certain machining operations [1].

For some types of machining, the workpiece–machine link provided by the chuck alone is incapable of sustaining the loads due to cutting and, in this case, using a tailstock centre remains indispensable. However, in many instances of turning, using a tailstock centre mainly allows the workpiece–machine assembly to be rigidified to allow the tolerances imposed by the Design Office to be respected, especially in terms of surface condition and geometric tolerance [1]. Machining a slender workpiece by turning with the workpiece being held by jaws on one side only is thus a delicate matter, both in the domains of strong and

weak cutting conditions. Indeed, machining operations implemented under blank cutting conditions and significant loads lead to workpiece flexures that adversely affect the geometric quality of the workpiece. These geometric defects can be significant enough to prevent a grinding phase being implemented directly. However, machining operations implemented in finishing cutting conditions do not allow surface conditions as determined by predictive models to be obtained, this being a function of the feed rate and the tool corner radius [2]. Indeed, the workpiece's low rigidity and its assembly often cause vibrations that interfere with machining [3,1].

In most cases, a setting workpiece is machined in order to determine the optimum values for tool offsets allowing machining defects to be compensated for as best as possible [4]. However, this method involves a major drawback, as it does not allow for due consideration of the fact that the amplitude of the defect generated by the workpiece flexure phenomenon is a function of the co-ordinates of the variable point machined. The correction made to the tool offset is limited to a mean defect correction. One alternative would involve machining with conditions generating significant tangential cutting force to limit vibrations of the workpiece and keep a good surface condition while following a path that compensates for workpiece flexure due to loads. This choice should allow us to respect the geometric specifications of the workpiece to be machined.

*

The goal of the present study is thus to characterise the behaviour of the workpiece and the workpiece–machine link in the case of turning for slender workpieces with held on one side only so as to be able to compensate for movements and deformations of workpieces during machining without a tailstock centre.

To do so, one can kit the machine up with instruments to measure workpiece flexure and process these data in real time within the control unit. However, this method cannot reasonably be considered in an industrial context [5]. The turning workpiece flexure phenomenon is taken into account by inserting offsets in the machining programme in order to best compensate the defect induced by workpiece flexure.

To model behaviour of the workpiece during machining, first a workpiece is machined so as to test validity of the model derived from the literature [6,7,4]. This model is commonly used to determine workpiece flexure during machining. Then, a new modelling is proposed for which the characteristics in relation to machining parameters are determined. To finish off, the validity of the proposed modelling is tested through additional machining operations.

The results derived from this modelling should allow for compensation of the defect due to workpiece flexure to be achieved at a low cost through performing early correction of the tool paths.

2. Experimental

2.1. Experimental procedure

A test workpiece (Fig. 1) was machined to implement measurements of flexure during machining without a tailstock centre. A measurement made during turning meant movement of the axis of seating B could be determined during machining of seating C.

The workpiece was produced on an NC lathe with power on the spindle of 11 kW and equipped with an NUM NC control unit. The chuck was equipped with three hard jaws and clamping pressure set to 5.5 bar for the entire duration of the test (clamping force: 1718 N). Flexure data acquisition was conducted using two Foucault current contact-free distance sensors with a resolution of 6.47 V/mm (measurement range of 3 mm) coupled with a memory multimeter whose maximum frequency of acquisition at full resolution is 40 Hz. The sensor was secured to the machine frame, then calibrated on the test workpiece. The position of the sensors on the Z-axis is noted “K” (Fig. 2) and the direction of measurement of the sensors corresponds to the directions of the lathe Y- and X-axis (directions of cutting load and radial cutting force). The machining loads were measured using an instrumented tool-holder with stress gauges calibrated at the start of the test campaign.

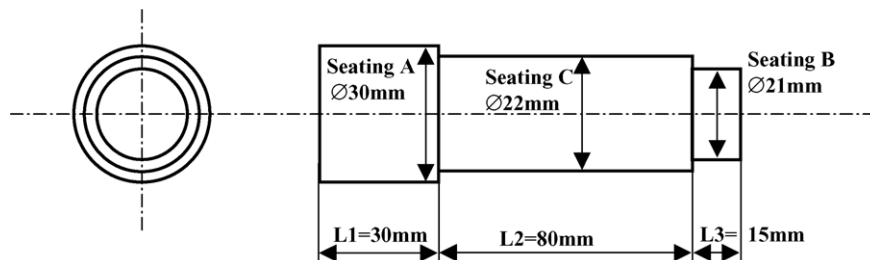


Fig. 1. Test workpiece set-up.

A comparator placed on the spindle allowed us to check that its movement remained within less than 3 μm during application of a load of 1500 N. This meant the spindle flexure phenomenon could be neglected during this study [4].

The workpiece was machined in a single phase from a 2017 T4 aluminium blank in accordance with the procedure defined in Fig. 2. The workpiece was held in the jaws throughout the length of seating A ($L_1 = 30$ mm).

The cutting conditions retained for the different operations are summarised in Fig. 2.

The tool used to produce the workpiece was installed in the tool-holder so as to limit the overhang of the active part of the tool and thus best limit the tool flexure phenomenon [4]. Seating B was machined carefully during operations 1 and 2 (see Fig. 2) and served as a reference to measure workpiece flexure during machining. The sensors allowed the movement dx of the surface of seating B along the X-axis to be measured as well as movement dy of the surface of seating B along the Y-axis during machining of seating C. Movements dx and dy measured during operation 3 when producing the test workpiece are shown in Fig. 3.

Analysis of the distance sensor measurement results provides us with knowledge of the influence exerted by machining loads on flexure at the end of the workpiece. During machining of the test workpiece, the maximum movement of the workpiece exceeded 0.18 mm along the Y-axis. The tangential cutting forces measured during machining were:

Tangential cutting force: $F_y = 1440$ N.

Longitudinal cutting force: $F_z = 521$ N.

Radial cutting force: $F_x = 388$ N.

2.2. Analysis of results and application

2.2.1. Determining workpiece flexure from sensor measurements

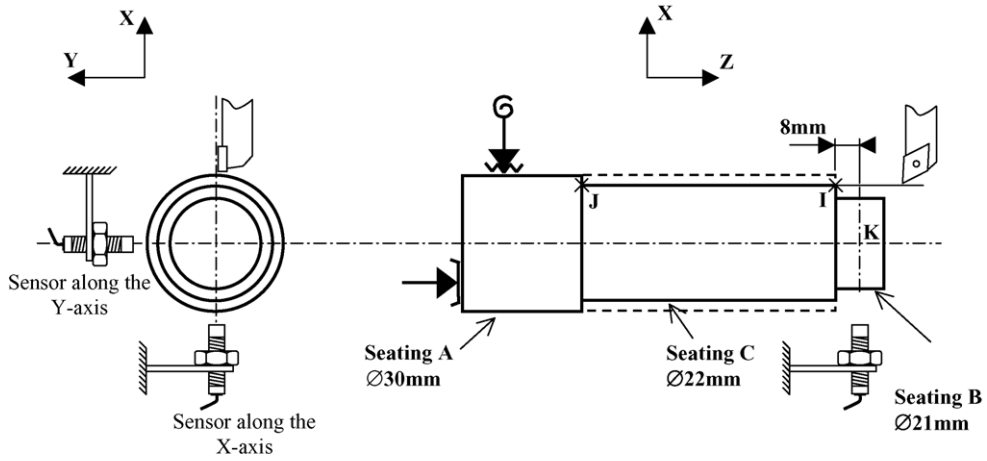
The abscissa $Z = 80$ mm (Fig. 3) corresponds to the start of operation 3 of workpiece machining (tool at point I, Fig. 2). Up to the abscissa $Z = 1$ mm (Fig. 3) corresponding to the end of operation 3 (tool at point J, Fig. 2), workpiece flexure diminished gradually as the tool moved closer to the spindle.

In light of the measurements shown in Fig. 3, it would appear that the movement measured along the X-axis is relatively insignificant compared with the movement measured along the Y-axis. Furthermore, the radial cutting force tends to make the workpiece bend towards the tool. This is due to the positive geometry of the tool used.

During machining, the position sensors meant movements dx and dy along the X- and Y-axis of the reference framework (G_0, X, Y) could be measured. Using these measurements, flexures f_x and f_y of the workpiece are determined in planes (X, Z) and (Y, Z) (Fig. 4). In a first approach, the amplitude of flexure of the tool is considered to be negligible in comparison with workpiece flexure.

The surface really generated considering deformations of the workpiece is a circle going through three points P_1, P_2 and P_3 of co-ordinates $(-R_0, 0)$, $(R_0 + dx, 0)$ and $(0, R_0 + dy)$ whose centre G_1 of co-ordinates (a, b) in the reference framework (G_0, X, Y) and radius R_1 verify the system of three equations with three unknowns below (Eq. (1)). Eq. (1) is a system of equations allowing the real surface machined to be defined.

$$\begin{cases} (-R_0 - a)^2 + b^2 = R_1^2 \\ (R_0 + dx - a)^2 + b^2 = R_1^2 \\ a^2 + (R_0 + dy - b)^2 = R_1^2 \end{cases} \quad (1)$$



Operation	Conditions	Tools
1- Machining of seating B - blank	$ap^* = 0.5\text{mm}$ $f^{**} = 0.07\text{mm/rev.}$ $Vc^{***} = 500\text{m/min}$	Tool DCGX 15 06 04-AL Tool-holder PDJNL 20-20
2- Machining of seating B - finishing	$ap = 0.5\text{mm}$ $f = 0.05\text{mm/rev.}$ $Vc = 600\text{m/min}$	
Timing, sprinkling and cooling of the workpiece Installation of sensors		
3- Machining of seating C	$ap = 4\text{mm}$ $f = 0.54\text{mm/rev.}$ $Vc = 250\text{m/min}$	Tool DCGX 15 06 04-AL Tool-holder PDJNL 20-20

(*) ap : depth of cut (**) f : feed rate (***) Vc : cutting speed

Fig. 2. Procedure.

Solving this system means values for a and b , co-ordinates of the centre of the real machined surface and its radius R_1 can be determined. The solution of the system of equations defining co-ordinates of the centre of the surface and the radius of the circle is presented below:

$$\begin{cases}
 a = \frac{dx}{2} \\
 b = \frac{dy^2 - R_0 \times dx + 2R_0 \times dy}{2(R_0 + dy)} \\
 R_1 = \sqrt{\left(R_0 + \frac{dx}{2}\right)^2 + \left(\frac{dy^2 - R_0 \times dx + 2R_0 \times dy}{2(R_0 + dy)}\right)^2}
 \end{cases} \quad (2)$$

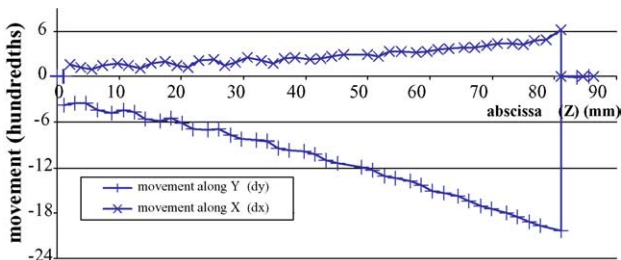


Fig. 3. Change in workpiece/sensor distances during machining of seating C.

According to the relations below (Eq. (3)), it is possible to determine the values for loads f_x and f_y as a function of movements dx and dy measured by the sensors and the radius R_0 of the programmed surface.

$$\begin{cases}
 R_0 = f_x + R_1 + a \\
 R_0 = R_1 - f_y + b
 \end{cases} \quad (3)$$

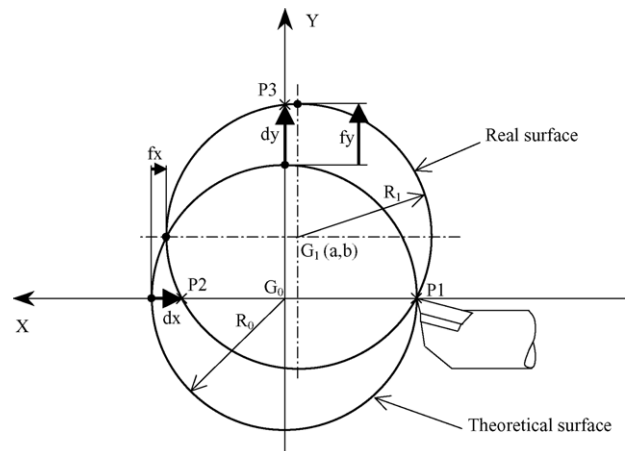


Fig. 4. Representation of theoretical and real surfaces machined during turning.

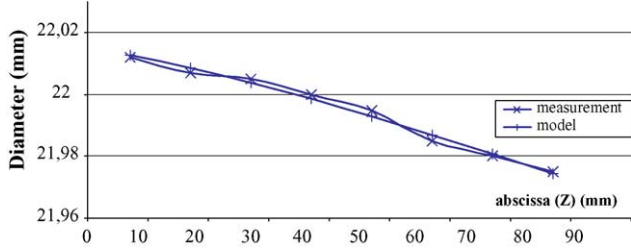


Fig. 5. Comparison between diameters measured and diameters measured on the test workpiece.

The relations introduced above (Eq. (4)) lead to the expression of loads f_x and f_y , respectively, along the X- and Y-axis induced by machining loads.

$$\begin{cases} f_x = R_0 - \sqrt{\left(R_0 + \frac{dx}{2}\right)^2 + \left(\frac{dy^2 - R_0 \times dx + 2R_0 \times dy}{2(R_0 + dy)}\right)^2} - \frac{dx}{2} \\ f_y = \sqrt{\left(R_0 + \frac{dx}{2}\right)^2 + \left(\frac{dy^2 - R_0 \times dx + 2R_0 \times dy}{2(R_0 + dy)}\right)^2} \\ + \frac{dy^2 - 2R_0^2 - R_0 \times dx}{2(R_0 + dy)} \end{cases} \quad (4)$$

2.2.2. Theoretical determination of the workpiece diameter

In order to validate the methodology for use of the results and the hypothesis whereby the amplitude of the tool flexure is negligible in comparison with workpiece flexure, it has been verified that the measurements dx and dy allow us to determine the real diameter of the machined workpiece. The theoretical radius R_1 of the machined workpiece is determined as a function of values dx and dy measured during the test (Eq. (2)).

Fig. 5 allows for a comparison of the results of diameter measurements made on the test workpiece and the theoretical results determined from values dx and dy measured during machining. The measurements for diameters of the workpiece with a given abscissa shown here are a mean for measurements calculated after a series of five measurements.

In the light of results from comparing the diameter measured on the workpiece and the diameter recalculated in accordance with movement measurements (Fig. 5), it appears that the maximum error committed on determination of the real diameter of the workpiece in accordance with the measurements made during the test does not exceed $3 \mu\text{m}$. It is thus possible to determine the diameter of the machined workpiece as a function of the abscissa Z from movement measurements during machining. Furthermore, this allows the assumption whereby tool flexure is negligible in comparison with workpiece flexure during machining to be validated.

3. Comparison with the model derived from the literature

To determine the workpiece flexure, the commonly accepted model [8] is derived from the theory of strength of materials shown in Fig. 6. In what follows, this model is called model 1.

The diameter of the beam under consideration is that of the workpiece before the tool cut. Indeed, the cross-section under stress is that located between point O (centre of the workpiece–chuck restraining bond) and the point of application of the load.

This study can be reduced to the case of a recessed beam under stress from deviated flexure. The workpieces for turning revolve around the Z-axis and all the direct orthonormed references containing the Z-axis are thus principal reference frameworks. The

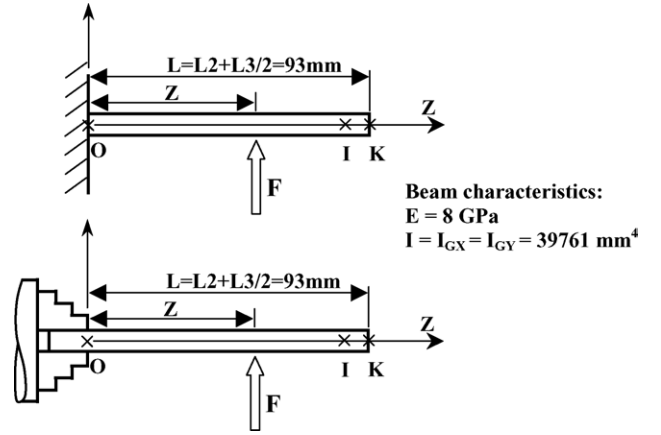


Fig. 6. Initial modelling of the workpiece during machining (model 1).

problem of flexure shown here can thus be studied separately in the planes (X, Z) and (Y, Z).

The static study performed on the modelling shown in Fig. 6 means that the expression for the deformation f_1 measured at point K can be determined as a function of the abscissa Z of the point of application of the load F and the various parameters characteristic of the beam. Deformations f_{1X} and f_{1Y} (Eq. (5)) are, respectively, caused by F_x and F_y along the X- and Y-axis. Expressions of deformations f_{1X} and f_{1Y} at point K under the action of loads F_x and F_y are presented below:

$$\begin{cases} f_{1X} = \frac{3L - Z}{6Z \cdot E \cdot I} \cdot F_x \cdot Z^3 \\ f_{1Y} = \frac{3L - Z}{6Z \cdot E \cdot I} \cdot F_y \cdot Z^3 \end{cases} \quad (5)$$

In Fig. 7, the theoretical loads calculated in accordance with modelling and the experimental loads calculated in accordance with Eq. (4) are compared. This comparison in each of the planes (X, Z) and (Y, Z) highlights the inadequacy of the model shown in Fig. 6 with respect to reality.

Now, the duration for machining of the test workpiece was less than 5 s. The results of works by Mize and Ziegert [9] as well as those of Lee et al. [10] allow us to assume that the influence of thermal phenomena remains negligible for the results of the tests. This is confirmed by the fact that the distance between the reference surface on the workpiece and the sensors remains the same before and after machining (without machining load).

The curve shapes for the experimental deformations of the workpiece along the directions X and Y are different from those

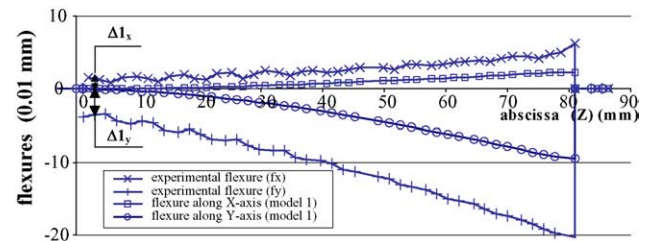


Fig. 7. Theoretical (f_1) and experimental values for deformation along the X- and Y-axis.

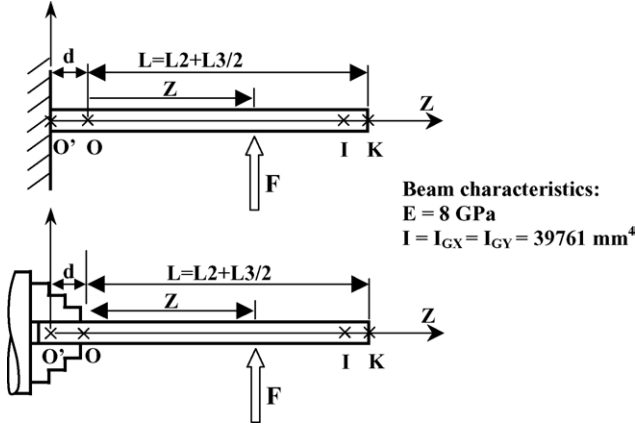


Fig. 8. Modified modelling (model 2).

derived from the modelling shown in Fig. 6. Offsets on the abscissa $Z=1$ (Fig. 7) appear between models and experimental measurements. They are noted as $\Delta 1_x$ and $\Delta 1_y$.

Oscillations of the curve of flexure along the X-axis could be due to machining vibrations, or to movements of the sensor support. A study is under way to determine the origin of the oscillations measured during the test. Considering the curve shapes for the experimental curves as compared with the curves from the model, it appears that the modelling initially proposed (Fig. 6) needs to be modified.

4. Modelling the workpiece flexure phenomenon

4.1. Proposal for new modelling

The presence of offsets $\Delta 1_x$ and $\Delta 1_y$ (Fig. 7) can be interpreted as an offset of the centre of the equivalent bond between the workpiece and the spindle in relation to the front side of the jaws. The big gap between the results of calculation for the workpiece deformation during machining from the standard beam model and experimental values led us to propose the modelling of Fig. 8. This model is called model 2.

In order to determine the position of the workpiece–spindle restraining bond, the parameter for offset of the restraining bond centre in relation to the front side of the jaws that is noted as d is introduced.

Deformations f_{2X} and f_{2Y} (Eq. (6)) are, respectively, induced by F_x and F_y along the X- and Y-axis.

Expressions of deformations f_{2X} and f_{2Y} at point K under the action of loads F_x and F_y are presented below:

$$\begin{cases} f_{2X} = \frac{3 \times (L + d) - (Z + d)}{6 \cdot E \cdot I} \cdot F_x \cdot (Z + d)^2 \\ f_{2Y} = \frac{3 \times (L + d) - (Z + d)}{6 \cdot E \cdot I} \cdot F_y \cdot (Z + d)^2 \end{cases} \quad (6)$$

Changes in the workpiece/sensor distances measured during machining of the test workpiece allow the value d of the restraining bond offset in relation to the front side of the jaws to be determined. This value is determined using the Excel software solver in accordance with the criterion for minimisation of the square root transformation of the deviations between experi-

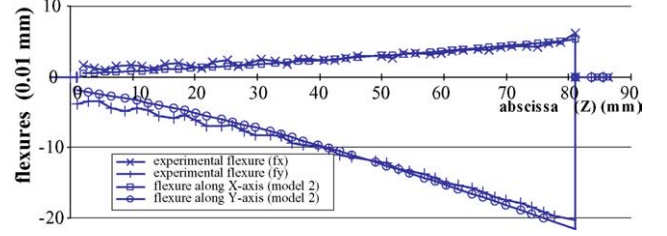


Fig. 9. Theoretical (f_2) and experimental values for the deformation along the X- and Y-axis.

mental values and theoretical values calculated from the second modelling.

The offset value d for modelling relative to the test is: $d = 31$ mm.

The graphs in Fig. 9 show the curves for change in workpiece flexure along the Y and X directions during the test, together with the theoretical trend curves determined from the modelling shown in Fig. 8 for an offset value d of 31 mm.

The curves represented in Fig. 9 show that introducing the parameter for offset of the restraining link centre means you can obtain much improved correlation between experimental measurements and modelling: the mean error is divided by 9 adopting the modelling that integrates an offset of the restraining centre.

The same offset value “ d ” allows you to obtain good correlation between experimental measurements and modelling results in the planes (X, Z) and (Y, Z). Additional analysis is thus implemented to validate the modelling proposed and allow the value of parameter d to be determined.

4.2. Validation of modelling proposed and calculation of the offset parameter

4.2.1. Choice of parameters for the study

In order to validate the modelling proposed in Fig. 8, the influence of certain parameters on the value for offset “ d ” of the modelling proposed is studied.

The influence of the following parameters is quantified:

Amplitude of loads applied to the workpiece during machining (factor F): In order to check that modelling is independent of the amplitude of machining loads, the influence of the “amplitude of machining loads” factor is quantified. Indeed, modelling must remain identical whatever the loading applied on the workpiece as long as the stresses imposed do not exceed the yield strength stress of the machined material.

Diameter of the machined workpiece (factor D): A change in the diameter of the machined workpiece also modifies the position of the points of contact between the workpiece and the jaws in the reference framework (O, X, Y, Z). This factor could have an influence on the position of the centre of reduction of the workpiece/spindle restraining bond.

Length of workpiece seized in the jaws (factor L): Just like the machined diameter, the length of the workpiece seized modifies the position of the points of contact between the workpiece and the jaws in the reference framework (O, X, Y, Z). This

Table 1
Summary of factors and values retained for tests

Factor	Low level	High level
Diameter	30 mm	50 mm
Load ^a	$F_y = 1440$ N and $F_x = 388$ N	$F_y = 720$ N and $F_x = 194$ N
Length of seizure	25 mm	39 mm
Pressure ^b	3 bar	5.5 bar

^a The values for loads efforts $F_y = 1440$ N and $F_x = 388$ N are obtained by performing a cut of 4 mm in depth at 0.54 mm/rev feed with a cutting speed of 250 m/min. Loads $F_y = 720$ N and $F_x = 194$ N are obtained by making a cut of 3 mm in depth at 0.36 mm/rev feed with a cutting speed of 250 m/min.

^b A pressure of 3 bar corresponds to a clamping load of 937 N on each of the jaws and a clamping pressure of 5.5 bar corresponds to a clamping load of 1718 N on each of the jaws.

parameter could have an influence on the position of the centre of reduction of the workpiece/spindle restraining bond.

Jaw clamping pressure (factor P): The jaw clamping pressure is adjustable using a pressure gauge on the test machine. Changing the clamping load of the workpiece can change the rigidity of the workpiece/spindle link and thus modify the parameter d for position of the centre of the equivalent restraining link.

For this first approach, the scope of this study is limited to one machine, one material and one type of jaw (hard jaws). Study of the effect of “machine”, “material” and “type of jaw” parameters may be considered within the scope of a broader study, in the light of the results from this first study.

4.2.2. Study of the influence of parameters by the experimental design method

4.2.2.1. *Defining the experimental design.* The values for the factors retained for this study are shown in Table 1.

A complete design for four factors on two levels in accordance with Table 2 is implanted, meaning that in principle, no interaction would be neglected. Furthermore, under reserve that the effects of the factors are linear, it is possible to write a raster model allowing for an interpolation of the results obtained over the range of variation for all the parameters.

Table 2
Table of tests from the test design

Test no.	Workpiece no.	Factor 1 (diameter)	Factor 2 (length)	Factor 3 (pressure)	Factor 4 (load)
1	5	30	25	3	1440
2	6	30	25	3	720
3	7	30	25	5.5	1440
4	8	30	25	5.5	720
5	1	30	39	3	1440
6	2	30	39	3	720
7	3	30	39	5.5	1440
8	4	30	39	5.5	720
9	13	50	25	3	1440
10	14	50	25	3	720
11	15	50	25	5.5	1440
12	16	50	25	5.5	720
13	12	50	39	3	1440
14	10	50	39	3	720
15	11	50	39	5.5	1440
16	9	50	39	5.5	720

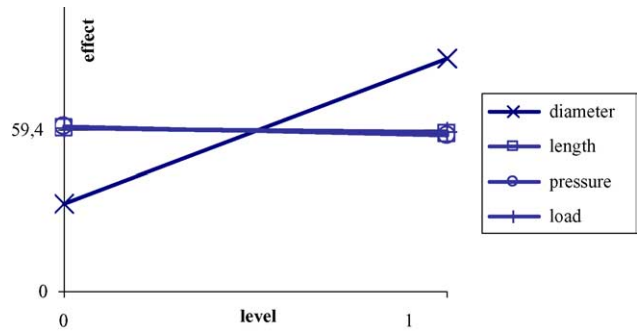


Fig. 10. Graph of effects of factors on parameter d .

Each of the tests was conducted in the same conditions (tool, material, machine and workpiece seizure) as for machining of the test workpiece (see set-up in Figs. 1 and 2). Only the values for the diameters of seatings A, B and C and the length L_1 change as a function of the levels of the factors.

4.2.2.2. *Analysis of results.* Measurements of the movements dx and dy along the X- and Y-axis and the loads F_x and F_y during machining allow us to determine the optimum value of parameter d . For each of the tests, the value for offset d retained is that which minimises the square root transformation of the offsets between flexure calculated in accordance with measurements of movements and theoretical flexure from model 2 as shown in Fig. 8.

Determination of parameter d for each of the 16 tests allows the graph of effects (Fig. 10) and graphs of interactions for each of the factors (Fig. 11) to be plotted.

Analysis of the graph of effects means that only the “diameter” factor has an influence on parameter d for offset of the restraining link. The fact that the “load” factor has no influence on the value of parameter d means the relevance of modelling 2 proposed in Fig. 8 can be confirmed.

The graphs for interactions of the first order highlight the very low interactions between factors. In order to determine a simple model for characterisation of the value of parameter d ,

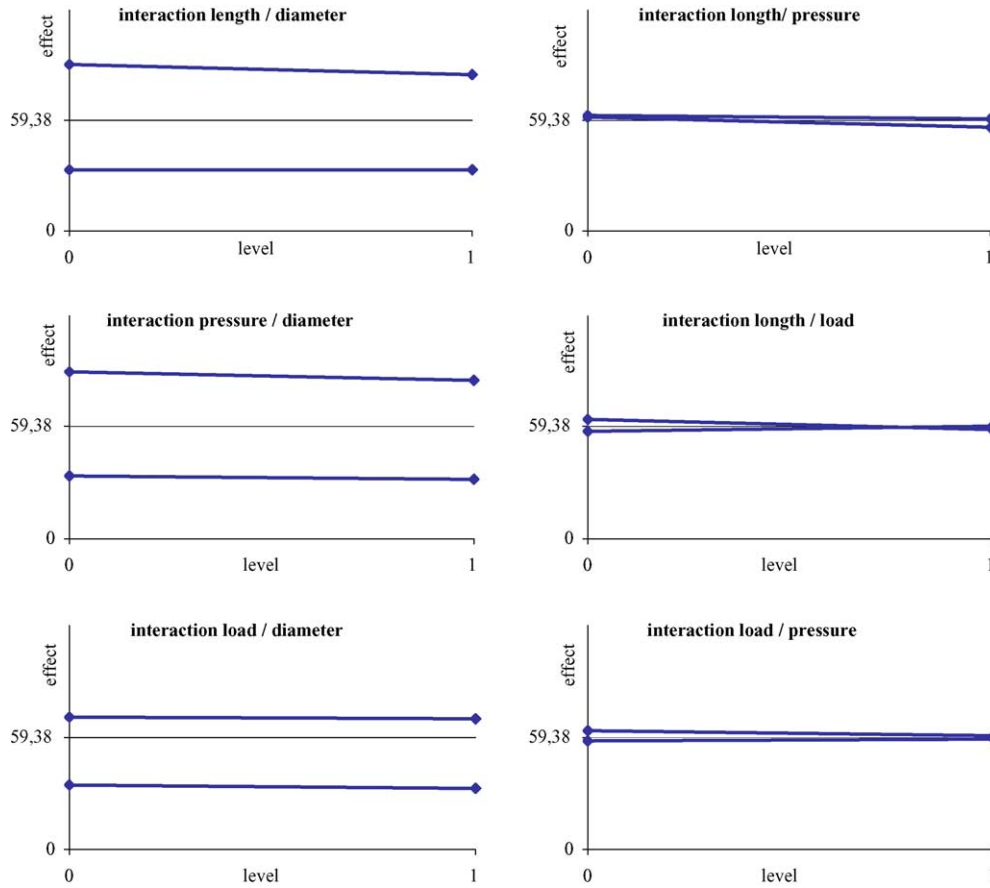


Fig. 11. Interaction graphs.

the change in this parameter is modelled solely as a function of the “diameter” factor. Interactions between the “diameter” and “pressure”, “diameter” and “length”, “diameter” and “load” factors are relatively insignificant and are neglected in this first approach.

Considering these assumptions, the raster model by Viguier and Sisson [11] offers an interpolation so that the value of parameter d at intermediate levels from those retained during the tests for the “diameter” factor can be determined. This formulation as a function of the results of tests from the experimental design and indicators for levels (InD1 and InD2) of the “diameter” factor is shown in Eq. (7) which presents a raster model for interpolation by Viguier and Sisson.

$$d = 59.39 + [-26.73 \quad 26.73] \begin{bmatrix} \text{InD1} \\ \text{InD2} \end{bmatrix} \quad (7)$$

$$\text{InD1} = \frac{\text{diameter} - 50}{30 - 50}$$

$$\text{InD2} = \frac{\text{diameter} - 30}{50 - 30}$$

For each of the workpieces produced, a comparison between the diameter measured and the diameter determined is made using the model introduced previously (Fig. 8). The diameters were measured every 10 mm along seating C (Fig. 2), that is eight measurement points per workpiece. Five series of measurements

per workpiece were made. The distribution of errors measured during the five series of measurements on the 16 test workpieces from the experiment design is illustrated in Fig. 12.

It appears that distribution of error on the sample studied can be assimilated to a normal distribution with standard deviation of 0.002 mm. This means the model’s uncertainty to ± 0.006 mm in relation to reality in 95% of cases.

With the raster model presented in Eq. (7), the value of the parameter d can be determined as a function of the diameter of the machined workpiece. This is valid under reserve that the

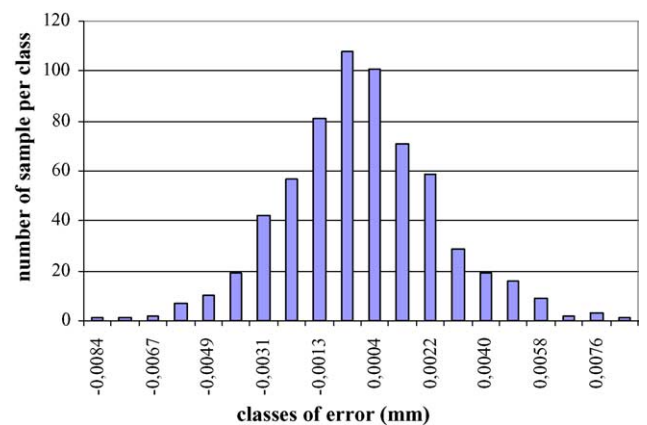


Fig. 12. Distribution of error between diameter measured and diameter determined with model 2.

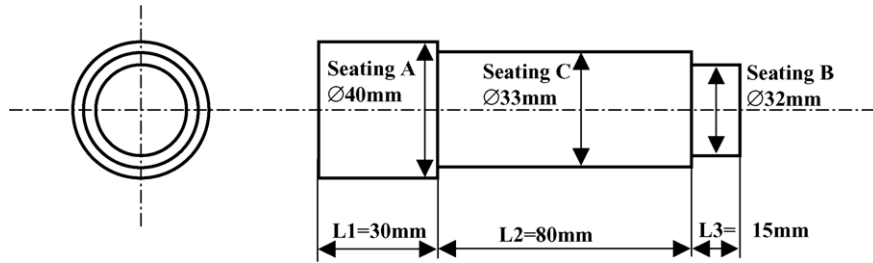


Fig. 13. Defining validation workpiece No. 1.

assumption of linearity of parameter d in relation to the diameter of the machined workpiece is satisfied.

5. Experimental verification of modelling

In order to apply the method for determination of workpiece flexure during machining using the new modelling, a workpiece is produced in conditions different from those retained for tests of the experimental design. This meant the validity of the raster formulation proposed (Eq. (7)) could be tested, as well as the linearity assumption for parameter d in relation to the diameter of the machined workpiece.

The machining of a workpiece made of 2017 T4 aluminium alloy whose definition drawing is shown in Fig. 13 is performed. Implementation, scheduling of machining operations, the tools and the machine used remain similar to those retained for the test workpiece and workpieces from the experimental design (Fig. 2).

The cutting parameters adopted to implement operation 3 are:

- $a_p = 3.5$ mm.
- $f = 0.45$ mm/rev.
- $V_c = 250$ m/min.
- Jaw clamping pressure = 4 bar.

These conditions led to the following loads, measured using the tool-holder equipped with instruments:

- Tangential cutting force: $F_y = 1010$ N.
- Longitudinal cutting force: $F_z = 371$ N.
- Radial cutting force: $F_x = 291$ N.

Considering the diameter of seating A, the raster model shown in Fig. 14 allows the value of parameter d for offset of

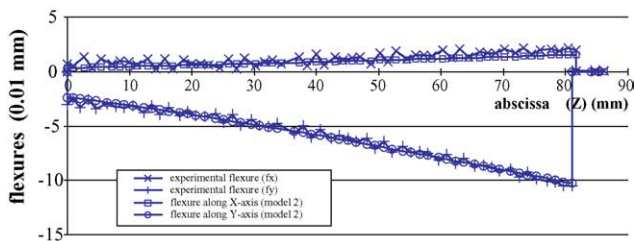


Fig. 14. Theoretical (f_2) and experimental values for the deformation along the X- and Y-axis.

the restraining link centre in relation to the front side of the jaws to be determined: $d = 59.39$ mm.

The graphs in Fig. 14 show the curves for changes in workpiece flexure along the directions Y and X during implementation of the validation workpiece, together with the curves for theoretical changes determined from the modelling shown in Fig. 8 with the value for offset set at 59.39 mm.

Correlation between the theoretical and experimental results checks the validity of the proposed model (Fig. 8). The assumption based on linearity of parameter d as a function of the “diameter” factor, as needed to write the raster model, is also verified (Eq. (7)) during this test.

6. Extrapolation in the case of another material

In order to test the validity of the modelling proposed for machining of different materials, the machining of a C40 steel workpiece with geometry similar to the previous workpiece is performed (see Fig. 13). Implementation, scheduling of machining operations and the machine used remain similar to those retained for the previous workpiece. The tools used involved a PDJNL 20-20 tool-holder and a DCMT 15 06 04-UF insert.

The cutting parameters adopted to implement operation 3 were:

- $a_p = 3.5$ mm.
- $f = 0.45$ mm/rev.
- $V_c = 250$ m/min.
- Jaw clamping pressure = 4 bar.

These conditions led to the following loads, measured using the tool-holder equipped with instruments:

- Tangential cutting force: $F_y = 903$ N.
- Longitudinal cutting force: $F_z = 402$ N.
- Radial cutting force: $F_x = 282$ N.

Considering the diameter of seating A, the raster model introduced in Eq. (7) can be used to determine the value of parameter d for offset of the restraining link centre in relation to the front side of the jaws: $d = 59.39$ mm.

The graphs in Fig. 15 show the curves for change in workpiece flexure along the Y and X directions during production of this steel workpiece, together with the theoretical trend curves determined the modelling shown in Fig. 8.

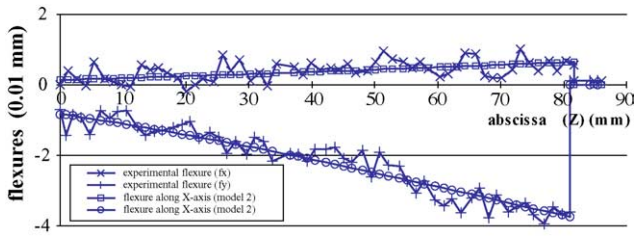


Fig. 15. Theoretical (f_2) and experimental values for the deformation along the X- and Y-axis.

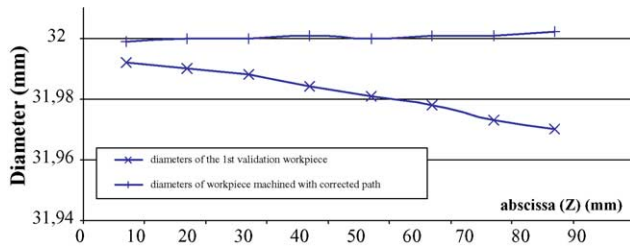


Fig. 16. Comparison of workpiece diameters with and without compensation of workpiece flexures.

Correlation between the theoretical and experimental results checks the validity of the proposed model (Fig. 8). The assumption based on linearity of parameter “ d ” needed to write the raster model is still verified (Eq. (7)). For this application, modelling thus proves to be independent of the machined material.

7. Example of application of automatic defect correction

A last workpiece made of 2017T4 aluminium alloy defined identically to the first validation workpiece was produced (see Section 5). Machining was implemented along a path that compensates the flexure due to machining loads in accordance with the modelling results (Fig. 8), while path correction was applied according to the mirror method [6,12,13] using the value of parameter d calculated using the raster model defined in Eq. (7).

Fig. 16 illustrates the diameters measured on the first application workpiece and those measured on the workpiece produced with a corrected path. These values are an average of the measurements calculated in accordance with a series of five measurements performed every 10 mm along the machined seating.

From the appearance of the curves in Fig. 16, it would appear that the error on the diameter of the machined seating is reduced from 22 μm to 3 μm taking the phenomenon of workpiece flexure during machining into account. To produce this workpiece, the proposed method thus allows for machining error in the diameter of the machined seating to be reduced by more than 85%.

8. Conclusion

This study’s aim is to propose a method for automatic correction of the path to machine slender workpieces.

Having tested the model commonly used to characterise the phenomenon of workpiece flexure during machining, a model

for workpiece flexure turning aluminium alloy with a given type of jaws is proposed. This model includes a parameter d for offset from the restraining link centre in relation to the front side of the jaws. Then, it is showed that this parameter is solely a function of the diameter of the machined workpiece. Experimental verification then enables us to validate the model proposed and machining with another material shows how this method can be extrapolated. Finally, machining with a path compensating for workpiece flexure is implemented. The example studied then shows the adequacy of the resolution method proposed to the problem posed by workpiece flexure during machining.

In the light of this study, that was limited to one type of material and one type of spindle, it appears possible to limit the defect due to workpiece flexure under the effect of loads due to cutting. This can be done by programming a corrected path compensating for workpiece flexure, for example, by carrying out a mirror type correction. This then releases us from the need to use the tailstock centre when the workpiece–spindle link alone is sufficient to sustain loads due to cutting. This method dispenses with the need to use sensors whose data would then have to be processed in real time and would need to be taken into account directly within the NC control unit. It is necessary to study validity of the modelling proposed for machines working on materials other than those to which this first study was limited.

References

- [1] B. Anselmetti, P. Bourdet, Optimisation of a workpiece considering production requirements, *Comput. Ind.* 21 (1993) 23–24.
- [2] W.S. Lin, B.Y. Lee, C.L. Wu, Modeling the surface roughness and cutting force for turning, *J. Mater. Process. Technol.* 108 (2001) 286–293.
- [3] E.C. Lee, C.Y. Nian, Y.S. Tarn, Design of a dynamic vibration absorber against vibrations in turning operations, *J. Mater. Process. Technol.* 108 (2001) 278–285.
- [4] C. Sandvik, *Techniques modernes d’usinage*, Impr. Tofters Tryckeri, 1997.
- [5] L. Chih-Hao, Y. Jingxia, N. Jun, An application of real-time error compensation on a turning center, *J. Mater. Process. Technol.* 35 (1995) 1669–1682.
- [6] G. Desein, *Qualification et optimisation de la précision d’une machine-outil à commande numérique*, Thèse de Génie Mécanique de l’Université Paul Sabatier, Toulouse, 1997.
- [7] J.R. Mayer, A.-V. Phan, G. Cloutier, Prediction of diameter errors in bar turning: a computationally effective model, *Appl. Math. Model.* 24 (October (12)) (2000) 943–956.
- [8] R. Ramesh, M.A. Mannan, A.N. Poo, Error compensation in machine tools—a review: Part I: geometric, cutting-force induced and fixture-dependent errors, *Int. J. Mach. Tools Manuf.* 40 (July (9)) (2000) 1235–1256.
- [9] C.D. Mize, J.C. Ziegert, Neural network thermal error compensation of a machining center, *Precision Eng.* 24 (October (4)) (2000) 338–346.
- [10] D.S. Lee, J.Y. Choi, D.-H. Choi, ICA based thermal source extraction and thermal distortion compensation method for a machine tool, *Int. J. Mach. Tools Manuf.* 43 (2003) 589–597.
- [11] M. Pillet, *Les plans d’expérience par la méthode Taguchi*, Les Edition d’organisation, 1997.
- [12] A. Larue, B. Anselmetti, Deviation of a machined surface in flank milling, *Int. J. Mach. Tools Manuf.* 43 (2003) 129–138.
- [13] T.I. Seo, *Intégration des effets de déformation d’outil en génération de trajectoires d’usinage*, Thèse de Doctorat de l’Université de Nantes et de l’Ecole Centrale de Nantes, Nantes, 1998.